



HAL
open science

Rheological evolution of straw-cattle manure (SCM) treated by dry anaerobic digestion in batch and in continuous pilot reactors

M.A. Hernandez-Shek, P. Peultier, A. Pauss, T. Ribeiro

► **To cite this version:**

M.A. Hernandez-Shek, P. Peultier, A. Pauss, T. Ribeiro. Rheological evolution of straw-cattle manure (SCM) treated by dry anaerobic digestion in batch and in continuous pilot reactors. *Waste Management*, 2022, 144, pp.411-420. 10.1016/j.wasman.2022.04.014 . hal-03673704

HAL Id: hal-03673704

<https://hal.science/hal-03673704>

Submitted on 22 Jul 2024

HAL is a multi-disciplinary open access archive for the deposit and dissemination of scientific research documents, whether they are published or not. The documents may come from teaching and research institutions in France or abroad, or from public or private research centers.

L'archive ouverte pluridisciplinaire **HAL**, est destinée au dépôt et à la diffusion de documents scientifiques de niveau recherche, publiés ou non, émanant des établissements d'enseignement et de recherche français ou étrangers, des laboratoires publics ou privés.



Distributed under a Creative Commons Attribution - NonCommercial 4.0 International License

1 **Rheological evolution of straw-cattle manure (SCM) treated by** 2 **dry anaerobic digestion in batch and in continuous pilot reactors**

3 M.A. Hernandez-Shek^{a,b,c}, P. Peultier^c, A. Pauss^b, T. Ribeiro^{a*}

4 ^aInstitut Polytechnique UniLaSalle, EA 7519 Transformations & AgroRessources, Rue Pierre Waguet, BP
5 30313, F-60026 Beauvais Cédex, France.

6 ^bAlliance Sorbonne Université, EA 4297 TIMR UTC/ESCOM, Université de technologie de Compiègne,
7 60203 Compiègne cedex, France.

8 ^cEasymetha, 6 rue des Hautes Cornes, 80000 Amiens, France.

9
10 *Corresponding author: Thierry Ribeiro; Tel.: +33 (0) 344 06 76 11; E-mail:

11 thierry.ribeiro@unilasalle.fr

12 **Abstract**

13 Knowledge of rheological evolution of biomass during dry anaerobic digestion (D-AD)
14 is important in the engineering design, modeling, and operation of D-AD reactors. In
15 this work, two methods of rheological analysis, the slump test and the shear-box, were
16 used to measure the evolution of the yield stress, cohesion and friction angle of the
17 straw-cattle manure (SCM) during the D-AD. Firstly, four 60 L batch leach-bed reactors
18 (LBR) were started in parallel and stopped at different stages of the D-AD process on
19 days 0, 10, 21 and 31. Secondly, a 500 L and 2 m length plug flow reactor (PFR) was
20 operated with 40 days of solid retention time and samples were recovered at different
21 positions. The solid degradation during D-AD process was monitored by analysis of the
22 degradation of volatile solids, the fiber content and the Flash BMP. Similar degradation
23 patterns of SCM and rheological evolution were observed in both reactors type. VS
24 content decreased of 10.7 % and 10.2 % in 30 days in PFR and LBR respectively. VS
25 degradation in both cases was well explained by hemicellulose and cellulose consuming
26 in D-AD process. Considering the rheological analysis, the results showed that D-AD
27 induced a reduction of the yield stress of 28.1 and 24.2 % in 30 days in PFR and LBR
28 respectively. Moreover, a similar evolution of cohesion and friction angle value for

29 samples from both reactors was observed. This study demonstrates the close
30 relationship between the state of degradation of the solid biomass and its rheological
31 properties.

32 **Keywords**

33 Rheology; Slump-test; Shear-box; Plug flow reactor; Leach-bed reactor; Ondalys Flash
34 BMP®

35 **1 Introduction**

36 Livestock is defined as the group of farm activities to raise useful animals to produce
37 commodities such as food, fiber, and labor. Manure is an unavoidable by-product of any
38 livestock production system, it represents a potentially important source of methane
39 emissions related to climate change ([Getabalew et al., 2019](#)). According to [Cheng et al.](#)
40 [\(2022\)](#), cattle and dairy manure accounts around 14.5 % of total planetary methane
41 (CH₄) emissions due to human activity. This situation becomes dramatic considering the
42 population growth which requires the intensification of animal husbandry. To avoid the
43 negative effects of methane release to the atmosphere livestock waste should be treated.

44 Anaerobic digestion (AD) is a biological process in which organic matter is transformed
45 under anoxic conditions by bacterial consortium into digestate and biogas (CH₄ and
46 CO₂) which is a renewable source of energy ([Gadaleta et al., 2021](#)). This process has
47 already proved its efficiency in the treatment and valorization of livestock wastes such
48 as manure and other agricultural by-products into biogas and digestate which could be
49 used as an organic fertilizer ([Guilayn et al., 2020](#)). Given the large physicochemical and
50 biological variability of manure, several AD processes have emerged for the sake of
51 offering a better handling option adapted to each livestock manure type. Livestock
52 manure could be classified either as liquid, slurry, semi-solid, or solid product as a

53 function of the total solids (TS) content and based on its mass flow and rheological
54 characteristics (Lague et al., 2005). From a rheological point of view, manure wastes
55 can be classified in those with Newtonian behavior ($< 5\%$ TS) such a liquid and
56 slurries, then, those products having a non-Newtonian behavior while increasing total
57 solids content ($5 - 15\%$ TS), and over 20% TS, solid manure has non-zero shear
58 strength as it can resist shear and move in bulk under the effect of a shear force
59 (Brambilla et al., 2013; Lague et al., 2005; Landry et al., 2004).

60 AD processes are classified according to the TS content of the biomass in wet anaerobic
61 digestion ($< 15\%$ TS) and Dry Anaerobic Digestion (D-AD) ($> 15\%$ TS) (Rocamora et
62 al., 2020). While the former is able to continuously produce biogas from manure
63 products with a liquid rheological behavior, the latter are specific to semi-solid and
64 solid wastes in batch or continuous systems in which pump and stirred systems could
65 not operate given the high viscosity and particle size of the products involved in the
66 process (André et al., 2018; Rocamora et al., 2020). Leach-bed reactor (LBR) working
67 in batch remains the most common D-AD technology, biogas production in batch
68 systems have found several drawbacks such as the irregular biogas flow and the high
69 demand for labor (Elsharkawy et al., 2019).

70 Continuous D-AD using horizontal PRF has been identified as promising technology in
71 order to implement D-AD with a continuous feeding (Dong et al., 2020, 2019; Patinvoh
72 et al., 2020, 2017). Industrial continuous D-AD reactors can be grouped according to
73 the method used to stir matter (mechanical and biogas recirculation) and by the way as
74 this is forwarded from the inlet to the outlet (compression, piston or gravity) (André et
75 al., 2018; Elsharkawy et al., 2019). High viscosity and low flowability medium have
76 been highlighted as a major issue for stirring and forwarding systems for continuous and
77 mixed D-AD reactors (Wu, 2014). Inspired by the Transpaille digester and the mass

78 movement experimented in biogas plants once batch reactors built as garages are open
79 ([Chiumenti et al., 2017](#)), the Easymetha technology devoid of mechanical or biogas
80 stirring seek to base its working on the fact of SCM rheological properties are reduced
81 while this is anaerobically digested, raising therefore its flowability ([Peultier, 2016](#)).
82 However, to our knowledge, non-study addressed the rheological evolution of SCM or
83 other coarse biomasses during D-AD. This could be explained by the lack of sustainable
84 rheometric equipment with the representative volume for coarse biomass. Thus,
85 rheological properties of manure wastes with coarse particles (>5 mm) in the semi-solid
86 and solid regime are not well documented in the literature. This is a limiting factor in
87 the design and determination of the energy requirements of matter displacement
88 operations within the continuous D-AD reactor ([Lague et al., 2005](#)).

89 In the last decade, efforts have been made to adapt and use alternative rheological
90 methods from other scientific knowledge to the characterization of solid biomass
91 present in D-AD process ([Benbelkacem et al., 2013a](#); [Garcia-Bernet et al., 2011](#)). Being
92 this the case of the slump test, the v-funnel and the shear-box equipment that has their
93 origins in the fresh cement and soil consistency analysis ([Fernandez et al., 2020](#); [Landry
94 et al., 2004](#)). However, the size of aggregates continues being larger in D-AD process
95 than the particles of some soils and cement; therefore, these alternative methods are still
96 limited to the characterization of SCM with fiber longer than 20 cm and digestates.
97 More recently, alternative rheological tools have been designed, built and validated for
98 the analysis of biomass with coarse particles; the consistometer, the slump test and the
99 shear-box ([Hernandez-Shek et al., 2021b](#)). The use of these devices for SCM and
100 digestate characterization might offer opportunities in determining the rheological
101 changes of coarse biomass treated in D-AD process.

102 Against this background, this study aims to: (1) determine and correlate the evolution of
103 the rheological and physical properties of SCM during D-AD process in batch and in
104 continuous reactors working at mesophilic temperature (37 °C); (2) verify the
105 hypothesis in which the rheological changes of the coarse biomass during D-AD would
106 facilitate its flow through continuous horizontal D-AD reactors avoiding the use of
107 mechanical moving parts inside the reactors; (3) introduce the use of alternative
108 methods to measure rheological changes of the coarse biomass. To do so, batch and
109 continuous reactors have been performed and sacrificed to recover samples with
110 different digestion time: In the first case, a PFR of 500 L and 2 m length was operated
111 in a continuous mode for two cycles of 40 days of solid retention time (SRT) and a
112 loading rate of 10 kg SCM day⁻¹, solid samples were collected at 0, 0.4, 1.1 , 1.7 and 2
113 m of length, equivalent approximately to 0, 8, 21, 34, 40 days of SRT. In the second
114 case, four batch reactors of 60 L (21 kg manure and 22 kg Inoculum) were started up in
115 parallel and stopped and sampled at different stages of AD process at days 0, 10, 21 and
116 31. Physical and rheological characterization was performed. Two rheological methods,
117 the slump test and the shear-box allowed to measure the evolution of the yield stress,
118 the cohesion, and the friction angle with the residence time in D-AD reactors. The
119 rheological results were contrasted with physical degradation measured by the volatile
120 solids, the fiber content (hemicellulose, cellulose, and lignin) and the Flash Biological
121 Methane Potential (BMP) values. This study expected to provide useful information for
122 engineers and biogas producers about the rheological and degradation state of coarse
123 biomass during D-AD in batch and in continuous reactors at different digestion times.

124

125

126

127 **2 Materials and methods**

128 *2.1 Substrate and inoculum collection*

129 The SCM was obtained from the dairy farm of the UniLaSalle Polytechnic Institute
130 located in Beauvais, France, with coordinates 49°27'58.2"N 2°04'17.5"E. In this farm,
131 the bedding material used was non-shredded wheat straw and the cow brand was Prim'
132 Holstein. Liquid inoculum was obtained from the liquid manure pit from the same farm.
133 No conservation of the tested materials was undertaken, they were directly characterized
134 and used in the D-AD reactors.

135 *2.2 Biomass physicochemical characterization*

136 For all the experiments, the total solids (TS) and volatile solids (VS) of the raw and
137 anaerobically digested biomass were determined according to [APHA standards \(2017\)](#).
138 Van Soest fractionation allowed the determination of the hemicellulose, cellulose and
139 lignin content, the test was performed in 70 °C dried and grinded samples ([van Soest,](#)
140 [1963](#)). Near Infrared Reflectance Spectroscopy (NIRS) was used for rapid
141 determination of the evolution of the biochemical methane potential (BMP). The
142 samples were dried at 70 °C for 5 days and grinded. A BUCHI NIR-Flex N-500 solid
143 spectrophotometer was used to scan each sample in reflectance over 1000-2500 nm,
144 with a resolution of 2.5×10^6 nm (Buchi®, Flawil, Switzerland). Each sample was
145 analyzed three times to evaluate homogeneity. Concerning the inoculum, the TS content
146 was measured at 1.9 % and the VS averaged 42.5 % TS. The pH was determined using
147 a pH meter (Mettler Toledo, Switzerland), the initial pH of the inoculum was 8.4. The
148 buffer capacity (TAC) and the volatile fatty acids (FOS) concentration were performed
149 by two acidification steps using sulfuric acid in an automatic titrator T50 (Mettler
150 Toledo, Switzerland) according to [Nordmann \(1977\)](#), the first acidification down to pH

151 5.0 allowed the TAC to be determined, and the second acidification down to pH 4.4
152 allowed the quantification of the FOS. The initial FOS/TAC ratio for the inoculum was
153 0.125.

154 *2.3 D-AD in pilot PFR*

155 2.3.1 Reactor design

156 PFR pilot was built in high-density polyethylene (HDPE) with a total volume of
157 approximately 0.65 m³ between the inlet (**Fig. 1**), the main and the outlet zones as
158 follows:

- 159 • Inlet zone

160 This part was provided with a sealed buffer system to avoid the release of gas and air
161 entering the system. This part can be considered as an inactive zone in the inlet system.
162 The total volume of the inlet is 32.8 L, the inlet storage volume is about with 20 L of
163 feedstock per feed. To ensure the feeding and the matter displacement in the reactor,
164 this zone is provided with an electric piston (MPO-WPC, MotionProPlus, France) with
165 600 mm of stroke length and a maximal load of 4,000 N over a surface of 0.4 x 0.14 m.

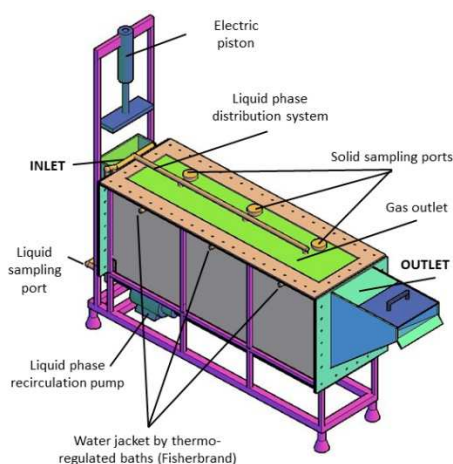
- 166 • Main zone

167 The main zone of the reactor has 2 m length, 0.6 m height and 0.4 m width. In this
168 section mesophilic conditions (37 °C) were maintained by recirculating water from
169 three thermo-regulated baths (Fisherbrand, France), through a water jacket (4 cm
170 thickness and capacity of 120 L) surrounding the main zone of the reactor. The reactor
171 was then shielded with a 40 mm Polystyrene surfaces to avoid heat loss. This zone was
172 able to produce biogas at working pressure between 13 and 15 mBar. The solid
173 substrate occupied a volume of approximately 436 L while the headspace was 40 L. A
174 perforated plate with 1 cm holes was located 10.0 cm up from the bottom of the reactor
175 to hold the solid substrate, thus creating a 71 L volume at the bottom of the reactors for

176 temporary liquid storage divided in three compartments. 10 L of leachate of each
177 compartment was mixed in a barrel and a centrifugal pump enabled the leachate
178 injection to the top of the solid material. A biogas circuit connected to the top of the
179 reactor to a volumetric drum biogas counter (TG, Ritter, Germany). Two ports, one on
180 the liquid and the other on the gas circuit, facilitated the collection of samples for
181 analysis. The composition of the biogas was monitored daily by a gas analyzer
182 (Multitec 540, Sewerin, France).

183 • Outlet zone

184 The material was transferred from the inlet towards the outlet at the end of the reactor
185 by the pressure force applied by the electric linear piston; as a result, the digested
186 residue was discharged through the outlet pipe while new materials were added. As in
187 the inlet zone, this part with sealed buffer system to avoid the release of gas and air
188 entering the system. Outlet zone has 64 L working volume. This zone is not heated, and
189 gas collection was not considered, thus, matter placed in this area is considered that its
190 digested cycle has finished. Digestate is manually removed from this zone while the
191 liquid phase is kept in the reactor to ensure the hydraulic seal and avoid gas leakage.
192 Liquid overflow was collected in a tank and reinjected to the system with each leachate
193 recirculation.



194

195 **Fig 1.** Schematic diagram and picture of developed pilot PFR for D-AD treatment

196 2.3.2 Experimental procedure

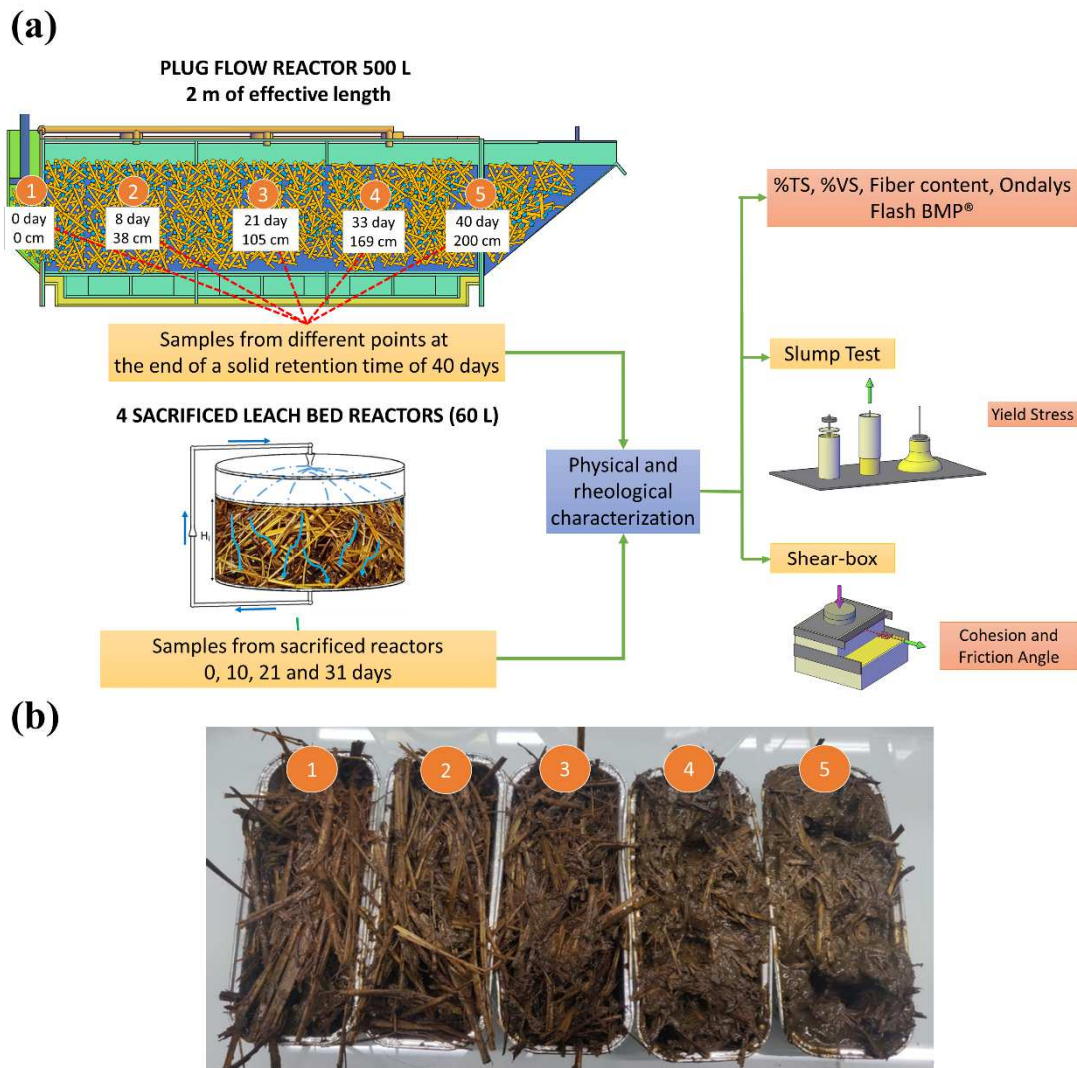
197 The experiment started in batch mode, first, 80 kg of water were added to fill the
198 leachate volume (80 L), once the bottom surface had a liquid sheet to flow, 209.5 kg
199 cattle manure was introduced combined with the 155 kg inoculum. The liquid fraction
200 ensured the hydraulic sealing of the PFR main zone and the immersion of the solid
201 phase. The calculated volatile solid ratio (VS substrate to VS inoculum) was 0.03 in the
202 reactor, this value was closed from that used by [Hernandez-Shek et al. \(2021a\)](#) in batch
203 immersed reactors of 2.4 m of height. In this batch, liquid and gas sealing, heating
204 systems, leachate recirculation systems and feeding piston working were tested. The
205 feeding of the empty reactor using the inlet systems allowed to study the initial
206 movement of solid and liquid phases in the reactor length, also to evidence the effect of
207 solid floating. Batch mode was kept for 34 days at 37 °C.

208 Once gas flow was less than 1 % of the cumulated biogas, two cycles with an organic
209 loading rate (OLR) of 1.43 kg_{VS} day⁻¹ and a 40 days of STR. To achieve these
210 conditions, the reactor was fed with 23.3 kg of cattle manure Monday, Wednesday and
211 Friday, getting approximately 70 kg week⁻¹ or 10 kg day⁻¹. Non-inoculum adding was
212 made in the continuous feeding mode, the liquid fraction inside the reactor would
213 inoculate the solid biomass. The digestate residue was withdrawn simultaneously with
214 the feeding keeping the hydraulic sealing in the inlet and in the outlet. The feeding
215 corresponds to approximately 5 piston drops. Once the reactor was fed and the digested
216 was removed, 30 kg of leachate (10 kg chamber⁻¹) was extracted from the bottom of the
217 reactor and mixed in an external barrel, then this volume was pumped to matter top.
218 Biogas flow and composition were continuously monitored. Process parameters, such as
219 pH, conductivity and VFA/ALK were measured with each feeding.

220 At the end of each cycle, samples were taken at different points of the main zone length
221 (**Fig. 2b**) and TS, VS, BMP and Van Soest analyses were performed. The rheology
222 measures (yield stress, cohesion, and friction angle) could only be performed in the
223 second digestion cycle, as the amount of sample necessary to perform analysis with the
224 slump test and the shear-box required the shutdown of the PFR (**Fig 2a**).

225 *2.1 D-AD in sacrificed batch LBR's 60 L*

226 Four batch reactors with liquid recirculation were started in parallel, and each was
227 sacrificed at different degradation stage after 0, 10, 21 and 31 days (**Fig 2a**). The
228 reactors used in this study were made of polyethylene; the internal diameter and the
229 total height were 39 cm and 50 cm, respectively, for a total volume of approximately 60
230 L. A mesh (5 mm holes) placed at the bottom avoided solid blockage of liquid phase
231 pipes recirculation. Twenty-one kilograms of SCM were gently placed in the reactor
232 using hands, subsequently, 22 kg of inoculum (liquid phase) was added obtaining a ratio
233 Inoculum/Substrate (I/S) of VS content equal to 0.05 according to [André et al. \(2015\)](#).
234 Reactors were hermetically sealed, and a thermostatically controlled water bad allowed
235 to keep mesophilic temperature (37 °C) during all the batch duration. Approximately 40
236 L of the liquid phase was daily recirculated (2 min each 2 h with a flow rate of 100 L h⁻¹)
237 ¹⁾ using MasterFlex peristaltic pumps. Once each reactor was stopped during the D-AD
238 process, samples were undertaken and TS, VS, van Soest, Ondalys Flash BMP® and
239 rheology (yield stress, cohesion and friction angle) were measured in order to
240 quantifying biomass degradation and physical and rheological changes.



241

242 **Fig. 2 (a)** Experimental set-up, sampling campaign and physical and rheological
243 analysis of raw SCM and digested samples

244 2.2 *Rheological characterization*

245 2.2.1 Slump test

246 The slump test consists of measuring the deformation of a material induced by gravity
247 and its own mass. Experiments were conducted over a high-density polyethylene (HD-
248 PE) surface (1 m²). A cylindrical PVC container (diameter 20 cm, height 34 cm, volume
249 10 L) was gently filled with the material to be analyzed. The container was quickly
250 raised allowing the collapse and deformation of the material. A disc plate (0.25 kg) of
251 the same diameter of the cylinder was used to avoid material stick to the cylinder

252 internal perimeter. All analyses were performed in duplicate. Yield stress was
253 determined using the slump height and the model equation developed by [Baudez et al.](#)
254 [\(2002\)](#). Further information on the slump test experimental devices is given by
255 [Hernandez-Shek et al. \(2021\)](#).

256 2.2.2 Shear-box

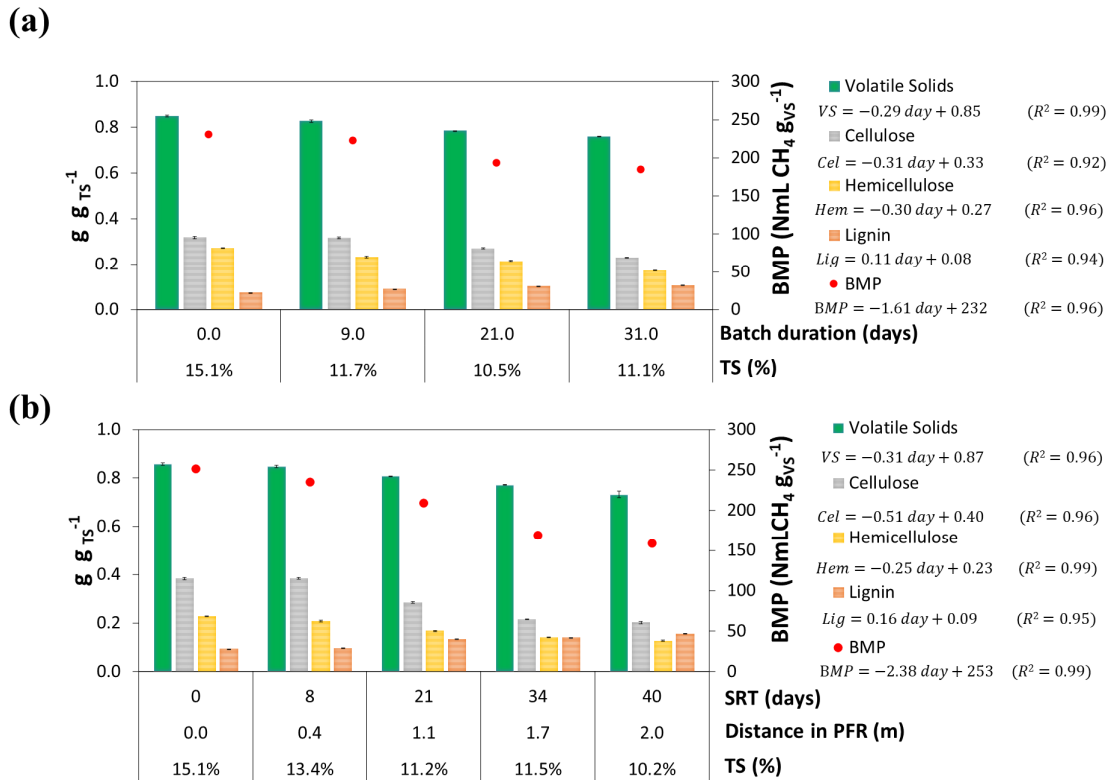
257 The shear-box consists of two independent rectangular half-boxes on a horizontal plane
258 which corresponds to the shear plane. Based on the device developed by [Bernard et al.](#)
259 [\(2016\)](#) A rectilinear shear-box has been built in our laboratory with a shear plane area of
260 0.5*0.3 m and 0.2*0.2 m ([Hernandez-Shek et al., 2021b](#)). The shear-box can operate in
261 samples from 10 to 60 L. A load cell (H3C3-500 kg) provided by ZEMIC has been used
262 connected to a RS232 receptor to register the changes in force during the shearing test.
263 Once installed, the shear-box is gently full using hands; the desire normal effort is
264 applied using disc weights until the desired surface sample pressure (0.1, 2, 4 and 6
265 kPa). A manual winch has been used to track the upper box and shearing the sample.
266 Experimental data were analyzed with Scilab 6.0 using a Gompertz equation. Maximal
267 shearing force at different normal pressures were used to construct the Mohr-Coulomb
268 breaking lines allowing the determination of the friction angle (φ) and the cohesion (c)
269 for each sample ([Miccio et al., 2013](#)).

270 3 Results

271 2.4 Physical characterization of SCM and digestates

272 The evolution of TS %, VS %, fibers and BMP for the SCM anaerobic digestion and
273 their linear regression parameters determining the kinetic degradation are shown in **Fig**
274 **3**. VS content decreased of 10.7 % and 10.2 % in 30 days in PFR and LBR respectively.
275 Similar VS degradation was determined by [André et al. \(2015\)](#) using sacrificed LBR for
276 the dry anaerobic digestion of SCM. As could be observed in **Fig. 3**, VS degradation in

277 both cases was well explained by hemicellulose and cellulose consuming during D-AD
 278 process. VS removal is explained by the hemicellulose and cellulose degradation in both
 279 reactors (Hernandez-Shek et al., 2020; Patinvoh et al., 2017).



280

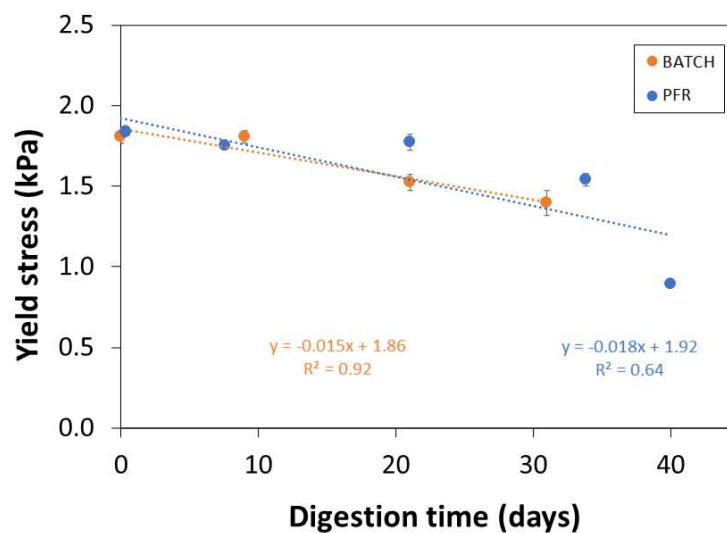
281 **Fig 3.** %TS, %VS, flash BMP and fiber content (hemicellulose, cellulose and lignin)
 282 evolution in sacrificed batch D-AD reactors (a) and in PFR (b) treating SCM

283 *2.5 Rheological characterization of SCM and digestates*

284 *2.5.1 Slump test results*

285 The yield stress evolution of SCM for samples from batch and continuous reactors is
 286 depicted in **Fig 4.** Yield stress was reduced in 24.2 % and 24.2 % in 30 days in PFR
 287 and LBR respectively (**Fig. 4**). For both reactor in the first 15 days, the value of yield
 288 stress did not present important variation, during this period hydrolysis and
 289 acidogenesis were performed and fiber content (hemicellulose and cellulose) remains
 290 similar (see **Fig. 3**). After day 15, once fiber degradation became more important, the
 291 yield stress of SCM was reduced from 1.8 to 1.5 Pa. This parameter linearly decreased

292 until day 31 in sacrificed LBR and until day 34 for continuous reactor, suggesting that
293 yield stress of SCM is highly correlated with the degradation state of the biomass. To
294 verify this correlation Pearson coefficient values and ANOVA analyses were
295 performed. The yield stress evolution was well correlated with the studied solid
296 degradation parameters and the time of solid anaerobic digestion, these coefficients
297 were higher than 0.90 for the sacrificed LBR (**Table 1**) and 0.74 for the PFR,
298 confirming the correlation between the yield stress and the degradation state of the
299 biomass. Hence, a higher solid retention time in D-AD implies higher reduction of the
300 apparent rheology and the physical properties of the solid biomass (Hernandez-Shek et
301 al., 2020).



302

303 **Fig 4.** Evolution of yield stress in sacrificed batch D-AD reactors and in PFR

304

305 **Table 1.** Linear regression comparing the results of yield stress with other measured
 306 parameters

Parameters	Coefficient R ²	p-value	Confidence level
VS	0.98	2.5E-02	95
Hemicellulose	0.90	1.0E-01	90
Cellulose	0.99	1.1E-02	95
Lignin	0.90	1.0E-01	90
BMP	0.98	1.5E-02	95
Macropores	0.94	6.3E-02	90
Mesopores	0.96	4.2E-02	95
Methane Yield	0.94	5.7E-02	90

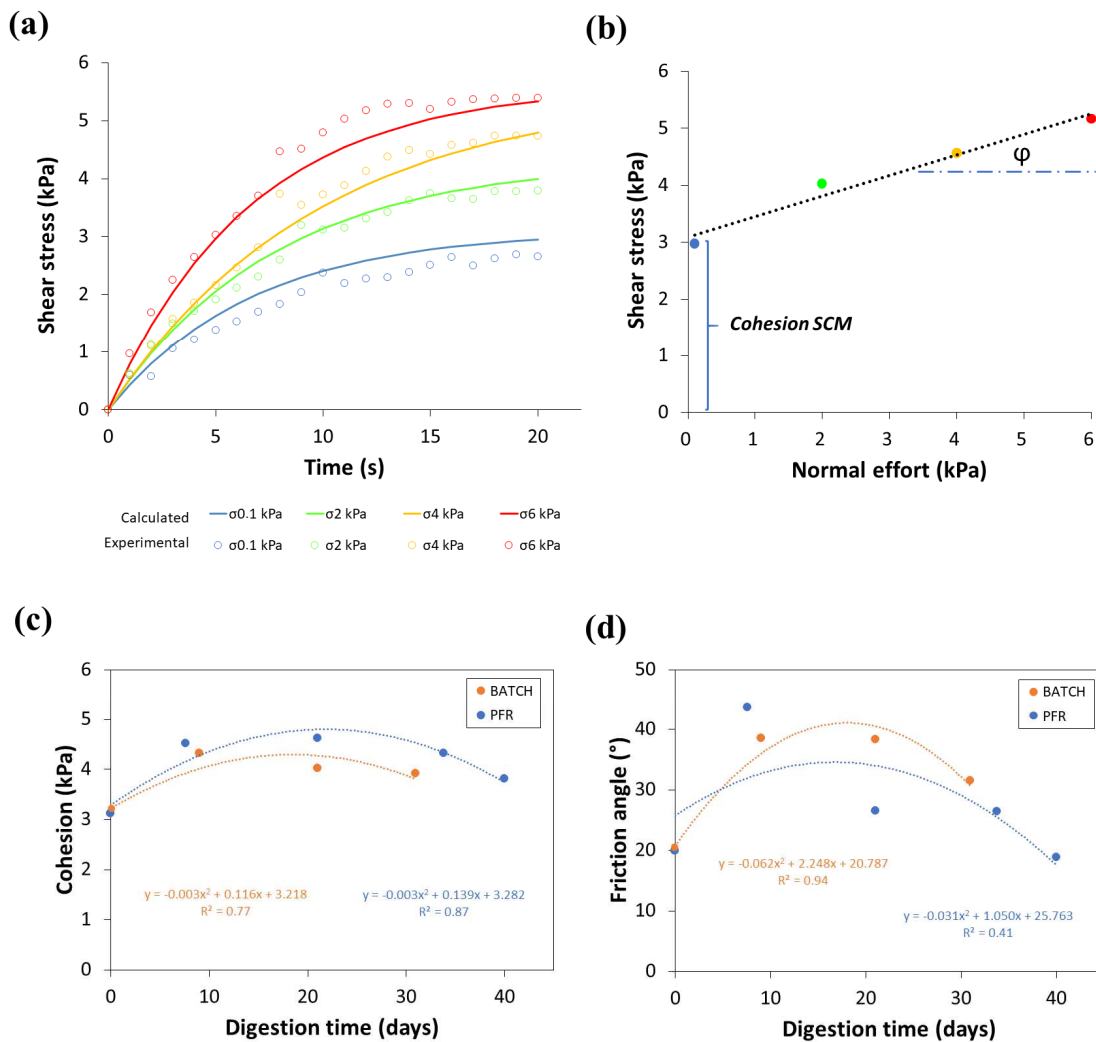
307

308 2.5.2 Shear-box results

309 Shear-box allowed the determination of cohesion and friction angles of the SCM and
 310 digested samples. Each sample was sheared under different normal efforts and the
 311 Mohr-Coulomb diagram allowed the determination of the cohesion and the friction
 312 angle; the shear results of SCM are depicted in **Fig. 5a** and **5b**. The values of shear
 313 strength at the different normal efforts for all samples, as well as the calculated values
 314 for cohesion and friction angle for all samples are presented in **Table 2**. As depicted in
 315 **Fig. 5c** and **Fig. 5d**, cohesion and friction angle are better fitted using 2nd degree
 316 polynomial equation rather than linear regression.

317 Cohesion and friction angle increased from 3 to 4 kPa and from 19.8 to 38.4°
 318 respectively in LBR since the begging of the batch until day 10. Similar observation
 319 was made for samples from the PFR, however, cohesion and friction angle increased in
 320 a higher degree in the PFR treatment between days 0 and 8, this could be explained by
 321 the pressure effect of the piston used to feed the reactor which can develop until 4,000
 322 N of force in the inlet zone allowing the displacement of matter inside the reactor likely
 323 when a toothpaste tube is squeezed. Few rheological changes were reported from days
 324 8 to 21 of samples from the PFR by the slump test and the shear-box; yield stress value

325 determined by the slump test remained closed to 1.7 kPa and cohesion value determined
 326 by shear-box was between 4.5 and 4.6 kPa. In both reactors after day 21, once fiber
 327 degradation became more important, the friction angle and cohesion values decreased
 328 (Fig 5).



329

330 **Fig 5.** (a) Shear test at different normal efforts of the SCM (b) Constructed Mohr-
 331 Coulomb failure diagram for SCM (b) cohesion evolution and (c) friction angle
 332 evolution during D-AD

333

334

	SCM	Sacrificed batch reactors			PFR			
	day 0	day 10	day 21	day 31	day 8 0.4 m	day 21 1.1 m	day 34 1.7 m	day 40 2 m
Normal Effort (kPa)	Shear strength (kPa)							
0.1	3.0	4.6	3.4	4.0	5.1	5.0	4.9	3.9
2.0	4.0	6.2	6.5	5.1	5.6	5.3	5.0	4.6
4.0	4.6	6.6	7.4	6.1	8.2	6.4	5.7	4.7
6.0	5.2	9.6	8.3	7.7	10.5	7.9	7.8	6.1
Mohr-Coulomb Linear Regression Results								
Cohesion (kPa)	3.1	4.3	4.0	3.9	4.5	4.6	4.3	3.8
Friction angle (°)	19.8	38.4	38.2	31.4	43.6	26.3	26.2	18.7
R²	0.97	0.91	0.89	0.99	0.94	0.94	0.88	0.82

335 **Table 2.** Experimental results obtained with the shear-box

336

337 *2.6 Biogas production in batch and PFR*

338 The continuous methane production is perhaps one of the most notorious advantages of
339 PFR operation over a batch one. Indeed, biomethane valorization systems such as
340 Coupled Heat-Power (CHP) units and natural gas grid injection requires uniform
341 conditions in methane production in terms of flow and composition. To ensure as much
342 as possible steady state in methane flow in batch operation, several reactors need to
343 work in parallel in different intervals of time. This operational condition requires a high
344 labor intensity to load and unload the reactors increasing in this way the operating cost
345 and limiting the options for automation of feeding and recovery of digestate (Chiumenti
346 et al., 2017). The biogas flow rate can follow extreme changes depending on the
347 behavior of each reactor, cogeneration systems are adapted to operate with a range of
348 flow rates, when the flow rate of biogas produced is higher than that of the CHP unit,

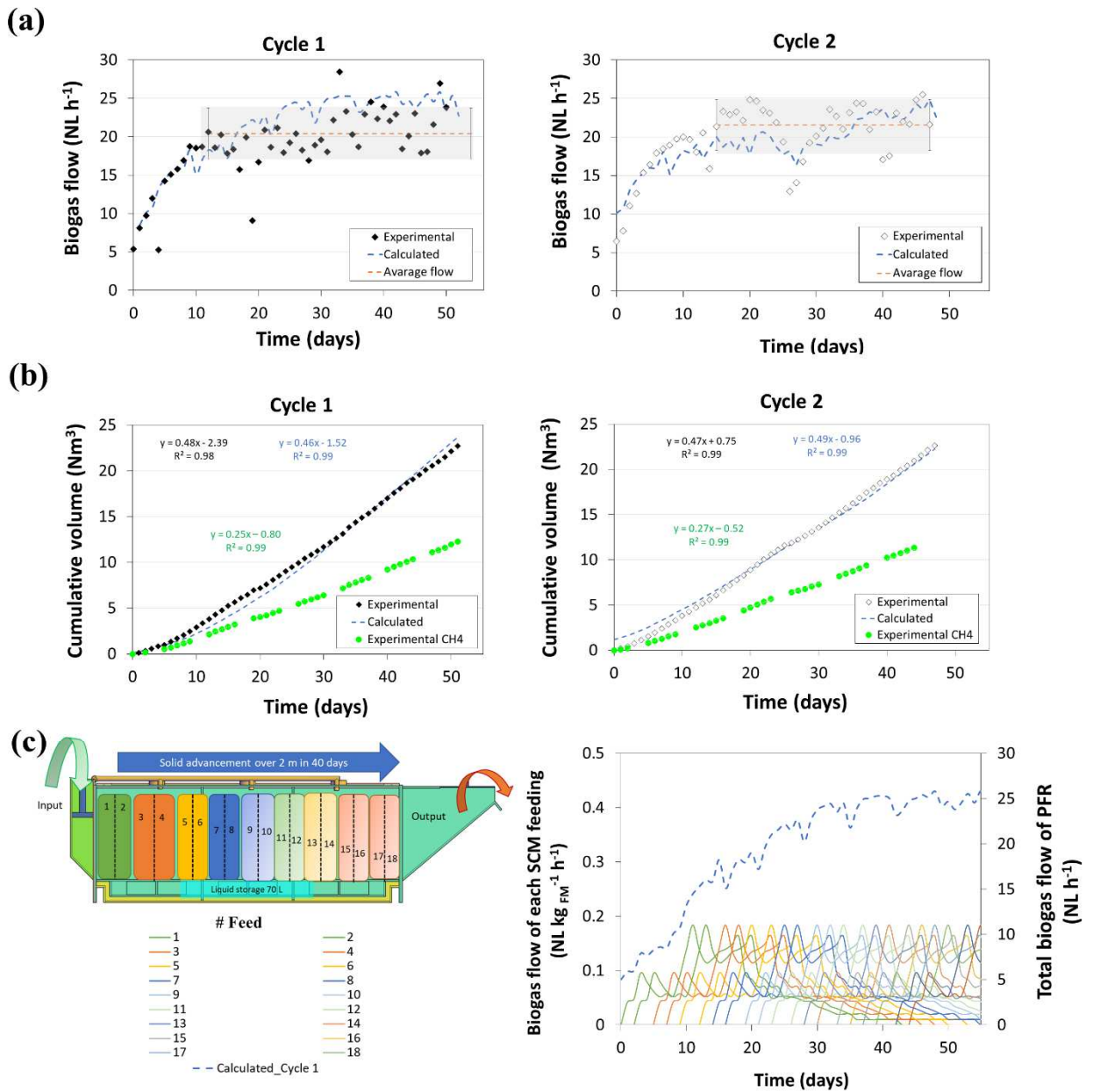
349 the excess volume of biogas produced during peak production is usually burned without
350 valorization (Riggio et al., 2017a).

351 Physical and rheological behavior have been shown a good correlation with the SCM
352 anaerobic degradation (**Table 1**); thus, biogas production is also related to these changes
353 inflicted to the biomass in D-AD. In this work biogas production from batch LBR
354 present similar behavior from those already described in the literature (André et al.,
355 2015; Chiumenti et al., 2017; Riggio et al., 2017a). As described by Hernandez-Shek et
356 al. (2020), the biogas production of D-AD batch reactor feed with SCM into mesophilic
357 conditions depicts one peak of dioxide carbon production around day 3, followed by
358 two peaks of methane production: the first presents between days 9 and 11, the second
359 peak was observed around 16 days after the reactor starting up. Comparing the
360 rheological characterization with the methane flow, it could be inferred that until the
361 first methane production peak the solid physical and rheological properties are mostly
362 influenced by the increase of water content instead of the solid structure destruction.
363 Indeed, during the first 10 days of D-AD, the hemicellulose was consumed in around
364 12% while the cellulose was barely degraded (**Fig. 3**). Once the second peak of biogas
365 production was overcome in LBR, the digestion achieved 28% of reduction of the
366 cellulose and therefore more important rheological changes.

367 Continuous gas production was enhanced in the PFR reactor using SCM as feed.
368 Contrasting rheological changes of SCM with its biogas production through anaerobic
369 digestion in PFR was not possible in this work. However, the similarities in biomass
370 degradation between sacrificed LBR and PFR suggest that solid retention time would
371 impact similarly the biogas production and thus the rheological properties of solid
372 biomass. The biogas flow per hour for both cycles is depicted in **Fig 6a**, steady state
373 was observed between days 12 and 57 for the first cycle and for the second one between

374 days 15 and 47. Average biogas flow at this time duration was 20.4 ± 3.3 and 21.6 ± 3.0
375 $\text{NL}_{\text{biogas}} \text{h}^{-1}$ for cycles 1 and 2 respectively. Biogas composition was measured along the
376 experiments, the system was sealed preventing oxygen from entering the system. The
377 average content of CH_4 was $54.1 \pm 2.1 \%$ and $53.6 \pm 1.5 \%$ in cycles 1 and 2
378 respectively. Cumulative biogas and methane production of PFR are shown in **Fig 6b**,
379 in LBR cumulated methane flow is usually simulated using exponential equations such
380 as Gompertz or first order kinetic equations ([Riggio et al., 2017b](#)). In continuous
381 methane production systems, the optimal case is to achieve a straight line in the
382 cumulated methane production (**Fig 6b**). This behavior was observed in both
383 experiments, slopes of methane production have similar values 0.46 and 0.49 and good
384 linear correlation is observed. Methane yield has been determined considering the
385 steady state of biogas flow (**Fig 6a**). Similar methane production was achieved by
386 [Patinvoh et al. \(2017\)](#) using a continuous mixed D-AD reactor of 4.7 L working volume
387 and feeding with shredded cattle manure and retention time of 40 days with a methane
388 production of $0.163 \text{ Nm}^3 \text{ CH}_4 \text{ kg}^{-1}\text{vs}$. Moreover, the recirculation and the immersion in
389 the liquid phase are special particularities of the developed reactor of this work.

390



391

392 **4 Discussion**

393 *4.1 Effect of solid degradation over the SCM rheological properties at different*
 394 *stages of D-AD in batch and PFR reactors*

395 The rheological behavior of biomass depends on the composition, the particle size and
 396 the physical properties (Dasari and Eric Berson, 2007; Hernandez-Shek et al., 2021b;
 397 Lam et al., 2008; Samaniuk et al., 2011). Considering the results of this work,
 398 rheological behavior is also function of the biomass degradation state. Yield stress

399 evolution with SRT was well correlated with fiber and VS degradation ($R^2 > 0.90$). This
400 means that SCM rheological behavior would progressively change from a porous elastic
401 solid behavior to one viscoelastic, similar conclusion was made by [Garcia-Bernet et al.](#)
402 [\(2011b\)](#) in the analysis of several digested solid wastes with particles inferior to 5 cm
403 size using the slump test with a lower volume of the sample chamber (**Fig. 3**).

404 The similarities in reduction of physical properties and the evolution of rheological
405 properties suggest that solid degradation is independent of the D-AD reactor type and
406 shows more dependency on the SRT or the batch duration. The use of linear parameters
407 in **Fig. 3** may allow the estimation of SCM degradation treated in D-AD reactors
408 working under liquid immersion and recirculation and at the mesophilic temperature.
409 Moreover, linear degradation of the SCM may confirm the lack of mixing of the solid
410 fraction in the axial direction of the reactor (forwards or backwards), which is a main
411 characteristic of PFR. In fact, in the designed PFR reactor the solid fraction would
412 progress from the inlet to the outlet behaving close to an ideal PFR reactor rather than a
413 series of complete stirred tank reactors as proposed by [Álvarez et al. \(2018\)](#) and
414 [Benbelkacem et al. \(2013\)](#) for the VALORGA process, which in contrast to developed
415 PFR in this study is equipped with biogas stirring and is used for shredded biomass D-
416 AD treatment under high digestate recirculation rate. Hence, the SCM degradation in
417 PFR could behave as a sequence of batch reactors in which each feeding is considered
418 as a new batch reactor launched inside the PFR, this hypothesis will be further discussed
419 in section 4.2 of this work.

420 The rheological properties as cohesion and friction angle are modified first by a higher
421 presence of water and then for fiber degradation while D-AD process is performed.
422 Considering sacrificed LBR, the water content increased from 81.4 % to 88.3 % in the
423 first 10 days of treatment and fiber content remained at similar values in the same

424 period, according to the shear test results, the water content could have increased the
425 cohesion and friction angle values (**Fig 5c**), similar changes are observed in sand, its
426 cohesion and friction angle increase when a certain amount of water is added allowing
427 the construction of a “sandcastle”. Another aspect to consider is the change of physical
428 properties such as bulk density and porosity. [Hernandez-Shek et al. \(2020\)](#) has reported
429 a reduction of the macropores volume from 30.4 to 19.8 % in the first 10 days of D-AD
430 process and to 1.7 % on day 31 of digestion. A decrease of macropores means that
431 spaces between particles are reduced by D-AD process, thus, particle friction is higher,
432 consequently, higher cohesion and friction angle values. According to [Hernandez-Shek
433 et al. \(2021a\)](#) the rheological changes and SCM anaerobic degraded might change
434 according to the position of the biomass in the solid bulk height and the management of
435 the liquid phase (immersion and recirculation). In this work, the rheological
436 characterization has been performed considering the digestion time in sacrificed LBR
437 and PFR, this means that the rheological changes are not only function on the position
438 of solid biomass inside the reactor but also dependent on the batch duration and the SRT
439 in continuous reactors.

440 Fiber degradation reduces friction, the SCM abrasiveness and the elasticity between
441 particles, and the digested material start to experiment more viscoplastic behavior
442 reducing the cohesion and the yield stress of the matrices. The final digested matter
443 obtained in the sacrificed LBR reactor at day 31 and in PFR at day 40 had similar
444 cohesion value, 3.8 and 3.9 kPa respectively (**Fig 5**). Generally, in a viscoplastic
445 behavior the deformations are no longer reversible as they could be elastic behavior,
446 once a shear stress higher than the yield stress is applied to the material flows like in
447 Bingham or Herschel-Bulkley fluid behavior ([Schneider and Gerber, 2020](#)); in contrast
448 to elastic behavior, the material would be compressed or stretched by the force without

449 showing a flow and the material could partially recover its initial state. Consequently,
450 the rheological changes inflicted to biomass by D-AD treatments while the organic
451 matter is degraded may have important implication in the operation of continuous D-
452 AD processes. In fact, these rheological changes accompanied by an increased water
453 content while D-AD is performed could facilitate the solid displacement in the PFR and
454 the transmission of momentum increase its ability to flow from the inlet to the outlet
455 under the pressure exerted by the piston feeder in the inlet zone. However, even if a
456 reduction of rheological properties of SCM is observed, the digestate still presents high
457 yield stress, cohesion, and friction values, thus, at the industrial scale it is necessary to
458 design special equipment as pumps or pistons to apply a shear force higher than its yield
459 stress value and forward solid matter inside the horizontal reactor.

460 *4.2 Implication of similarities of solid degradation and rheological changes in*
461 *continuous and discontinuous D-AD reactors on the comprehension of the*
462 *process*

463

464 Considering the similarities in SCM degradation and the evolution of rheological
465 properties in both batch and continuous D-AD reactor; in this section the biogas flow
466 behavior obtained in LBR was used to simulate that from the PFR according to its
467 feeding parameters (mass of SCM and frequency of feeding along the week: Monday,
468 Wednesday and Friday). In this scenario, a solid retention time of 40 days is composed
469 of 18 feeds of 23.3 kg_{FM} (**Fig 6c**). Considering the hypothesis in which, each of these
470 feeds is equivalent to the start-up of a batch reactor inside the continuous reactor, the
471 purpose here is to highlight the possibility of estimate biogas production of PRF from
472 LBR kinetics.

473 Assuming that the reactor is perfectly heated throughout the volume, and that there is no
474 variation in SCM composition or accumulation given the presence of dead flow zones,
475 **Fig. 6c** represents the methane flow of each feed and the daily sum would be equivalent
476 to the total methane flow in the reactor. The sum of the flows of the different SCM
477 feeds is represented in **Fig. 6a** for cycles 1 and 2 with the calculated data. The
478 experimental and cumulative biogas production is also shown in **Fig. 6a**. The
479 similarities between the experimental and calculated biogas flow production could
480 partially substantiate the above hypothesis that the PFR behaves as a sequence of batch
481 reactors. However, to fully verify this hypothesis and propose the use of existing models
482 describing the D-AD process, a solid residence time distribution (SRTD) analysis is
483 being performed to investigate the solid phase flow behavior inside the PFR. This study
484 could open up new possibilities for continuous D-AD modeling from batch data, which
485 are abundant in the literature. Therefore, a better understanding of the physicochemical
486 and biological principles of the PFR applied to the D-AD process of solid organic
487 wastes such as SCM.

488 **5 Conclusions**

489 Solid degradation is closely related with changes in the rheological properties while
490 biomass is treated by D-AD. Similar changes on SCM physical and rheological
491 properties were observed in both continuous and batch reactors. Thus, the rheological
492 changes depend on the biomass solid retention time inside the D-AD reactors rather
493 than the operation mode (continuous and discontinuous). The reduction of rheological
494 properties of SCM enhanced by biological fiber destruction could facilitate the
495 industrial operation of continuous D-AD reactors. However, the PFR operation
496 demonstrated that even if some rheological properties were reduced through D-AD
497 process, the digestate still presents high yield stress, cohesion, and friction values, thus,

498 at the industrial scale it is necessary to design special equipment to apply a shear force
499 higher than its yield stress value and forward solid matter inside the horizontal reactor.
500 The rheological properties measured in this work could be useful in the calibration and
501 the development of physical models able to describe the movement and energetic
502 balances in the operation of continuous D-AD digesters treating coarse biomass.

503 The rheological parameters of SCM and digestates were successfully determined by the
504 slump test and the shear-box methods. These alternative rheological tools were
505 successful for the determination of the rheological properties of coarse biomass in D-
506 AD plants avoiding the transport of high-volume samples until a laboratory. Moreover,
507 the use of these devices could help in the identification and preparation of the optimal
508 biomass mixtures having the desired rheological properties to facilitate the solid
509 displacement, avoid solid/liquid segregation, solid settlement, and the formation of dead
510 volumes.

511 Finally, the similarities between the solid degradation and the biogas production from
512 batch and continuous D-AD reactors of this work could represent an advancement in the
513 comprehension, design and modelling of industrial D-AD continuous processes. To
514 corroborate this fact, a SDTS must be performed to give a classify the PFR developed in
515 this work as a series of batch reactors.

516 **3 Acknowledgments**

517 The authors wish to thank the Association Nationale Recherche Technologie (ANRT)
518 for the financial support of this work and for the Ph.D. grant of Manuel HERNANDEZ-
519 SHEK (CIFRE n° 2017/0352). For their help in the fiber and flash BMP analysis special
520 thanks to Laura André.

521 **4 References**

- 522 Álvarez, C., Colón, J., López, A.C., Fernández-Polanco, M., Benbelkacem, H., Buffière,
523 P., 2018. Hydrodynamics of high solids anaerobic reactor: Characterization of
524 solid segregation and liquid mixing pattern in a pilot plant VALORGA facility
525 under different reactor geometry. *Waste Manag.* 76, 306–314.
526 <https://doi.org/10.1016/j.wasman.2018.02.053>
- 527 André, L., Durante, M., Pauss, A., Lespinard, O., Ribeiro, T., Lamy, E., 2015.
528 Quantifying physical structure changes and non-uniform water flow in cattle
529 manure during dry anaerobic digestion process at lab scale: Implication for biogas
530 production. *Bioresour. Technol.* 192, 660–669.
531 <https://doi.org/10.1016/j.biortech.2015.06.022>
- 532 André, L., Pauss, A., Ribeiro, T., 2018. Solid anaerobic digestion: State-of-art, scientific
533 and technological hurdles. *Bioresour. Technol.* 247, 1027–1037.
534 <https://doi.org/10.1016/j.biortech.2017.09.003>
- 535 APHA, 2017. Standard methods for the examination of water and wastewater, 23rd ed,
536 American Public Health Association. Inc. Washington, DC.
- 537 Baudez, J.C., Chabot, F., Coussot, P., 2002. Rheological interpretation of the slump test.
538 *Appl. Rheol.* 12, 133–141.
- 539 Benbelkacem, H., Garcia-Bernet, D., Bollon, J., Loisel, D., Bayard, R., Steyer, J.P.,
540 Gourdon, R., Buffière, P., Escudié, R., 2013a. Liquid mixing and solid segregation
541 in high-solid anaerobic digesters. *Bioresour. Technol.* 147, 387–394.
542 <https://doi.org/10.1016/j.biortech.2013.08.027>
- 543 Benbelkacem, H., Garcia-Bernet, D., Bollon, J., Loisel, D., Bayard, R., Steyer, J.P.,

544 Gourdon, R., Buffière, P., Escudié, R., 2013b. Liquid mixing and solid segregation
545 in high-solid anaerobic digesters. *Bioresour. Technol.* 147, 387–394.
546 <https://doi.org/10.1016/j.biortech.2013.08.027>

547 Bernard, A., Peyras, L., Royet, P., 2016. L’essai de cisaillement à la grande boîte de
548 Casagrande : un banc expérimental pour évaluer les propriétés des sols grossiers et
549 pour d’autres applications en géomécanique. *Rev. Fr. géotechnique* 146, 4.
550 <https://doi.org/10.1051/geotech/2016004>

551 Brambilla, M., Romano, E., Cutini, M., Pari, L., Bisaglia, C., 2013. Rheological
552 properties of manure/biomass mixtures and pumping strategies to improve
553 ingestate formulation. *Am. Soc. Agric. Biol. Eng.* 56, 1905–1920.

554 Cheng, M., McCarl, B., Fei, C., 2022. Climate Change and Livestock Production: A
555 Literature Review. *Atmosphere* (Basel). 13.
556 <https://doi.org/10.3390/atmos13010140>

557 Chiumenti, A., da Borso, F., Limina, S., 2017. Dry anaerobic digestion of cow manure
558 and agricultural products in a full-scale plant: Efficiency and comparison with wet
559 fermentation. *Waste Manag.* 71, 704–710.
560 <https://doi.org/10.1016/j.wasman.2017.03.046>

561 Dasari, R.K., Eric Berson, R., 2007. The effect of particle size on hydrolysis reaction
562 rates and rheological properties in cellulosic slurries. *Appl. Biochem. Biotechnol.*
563 137–140, 289–299. <https://doi.org/10.1007/s12010-007-9059-x>

564 Dong, L., Cao, G., Guo, X., Liu, T., Wu, J., Ren, N., 2019. Efficient biogas production
565 from cattle manure in a plug flow reactor: A large scale long term study.
566 *Bioresour. Technol.* 278, 450–455. <https://doi.org/10.1016/j.biortech.2019.01.100>

567 Dong, L., Cao, G., Tian, Y., Wu, J., Zhou, C., Liu, B., Zhao, L., Fan, J., Ren, N., 2020.
568 Improvement of biogas production in plug flow reactor using biogas slurry
569 pretreated cornstalk. *Bioresour. Technol. Reports* 9.
570 <https://doi.org/10.1016/j.biteb.2019.100378>

571 Elsharkawy, K., Elsamadony, M., Afify, H., 2019. Comparative analysis of common
572 full scale reactors for dry anaerobic digestion process. *E3S Web Conf.* 8.
573 <https://doi.org/10.1051/e3sconf/20198301011>

574 Fernandez, H.C., Ramirez, D.A., Franco, R.T., Buffière, P., Bayard, R., 2020. Methods
575 for the evaluation of industrial mechanical pretreatments before anaerobic
576 digesters. *Molecules* 25, 1–14. <https://doi.org/10.3390/molecules25040860>

577 Gadaleta, G., De Gisi, S., Notarnicola, M., 2021. Feasibility analysis on the adoption of
578 decentralized anaerobic co-digestion for the treatment of municipal organic waste
579 with energy recovery in urban districts of metropolitan areas. *Int. J. Environ. Res.*
580 *Public Health* 18, 1–17. <https://doi.org/10.3390/ijerph18041820>

581 Garcia-Bernet, D., Loisel, D., Guizard, G., Buffière, P., Steyer, J.P., Escudie, R., 2011.
582 Rapid measurement of the yield stress of anaerobically-digested solid waste using
583 slump tests. *Waste Manag.* 31, 631–635.
584 <https://doi.org/10.1016/j.wasman.2010.12.013>

585 Getabalew, M., Alemneh, T., Akebereg, D., 2019. Methane Production in Ruminant
586 Animals: Implication for Their Impact on Climate Change. *Concepts dairy Vet.*
587 *Sci.* 204–211. <https://doi.org/10.32474/CDVS.2019.02.000142>

588 Guilayn, F., Rouez, M., Crest, M., Patureau, D., Jimenez, J., 2020. Valorization of
589 digestates from urban or centralized biogas plants: a critical review, *Reviews in*

590 Environmental Science and Biotechnology. Springer Netherlands.
591 <https://doi.org/10.1007/s11157-020-09531-3>

592 Hernandez-Shek, M.A., André, L., Peultier, P., Ribeiro, T., Pauss, A., 2021a.
593 Immersion Effect on the Anaerobic Degradation and the Rheological Properties of
594 Straw - Cattle Manure (SCM) at 440 L Batch Pilot Scale Reactor. Waste and
595 Biomass Valorization. <https://doi.org/10.1007/s12649-021-01458-2>

596 Hernandez-Shek, M.A., Mathieux, M., André, L., Peultier, P., Pauss, A., Ribeiro, T.,
597 2020. Quantifying porosity changes in solid biomass waste using a disruptive
598 approach of water retention curves (WRC) for dry anaerobic digestion. Bioresour.
599 Technol. Reports 100585.
600 <https://doi.org/https://doi.org/10.1016/j.biteb.2020.100585>

601 Hernandez-Shek, M.A., Mottelet, S., Peultier, P., Pauss, A., Ribeiro, T., 2021b.
602 Development of devices for the determination of the rheological properties of
603 coarse biomass treated by dry anaerobic digestion.
604 <https://doi.org/10.1016/j.biteb.2021.100686>

605 Lague, C., Landry, H., Roberge, M., 2005. Engineering of land application systems for
606 livestock manure: A review. Can. Biosyst. Eng. 47, 617–628.

607 Lam, P.S., Sokhansanj, S., Bi, X., Lim, C.J., Naimi, L.J., Hoque, M., Mani, S., Womac,
608 A.R., Ye, X.P., S., N., 2008. Bulk density of wet and dry wheat straw and
609 switchgrass particles. Appl. Eng. Agric. 24, 351–358.
610 <https://doi.org/10.13031/2013.24490>

611 Landry, H., Lague, C., Roberge, M., 2004. Physical and rheological properties of
612 manure products. Appl. Eng. Agric. 20, 277–288.

613 Miccio, F., Barletta, D., Poletto, M., 2013. Flow properties and arching behavior of
614 biomass particulate solids. *Powder Technol.* 235, 312–321.
615 <https://doi.org/10.1016/j.powtec.2012.10.047>

616 Nordmann, W., 1977. Die Überwachung der Schlammfäulung. KA-Informationen für
617 das Betriebspersonal. Beilage zur Korrespondenz Abwasser 3/77.

618 Patinvoh, R.J., Kalantar Mehrjerdi, A., Sárvári Horváth, I., Taherzadeh, M.J., 2017. Dry
619 fermentation of manure with straw in continuous plug flow reactor: Reactor
620 development and process stability at different loading rates. *Bioresour. Technol.*
621 224, 197–205. <https://doi.org/10.1016/j.biortech.2016.11.011>

622 Patinvoh, R.J., Lundin, M., Mohammad, ., Taherzadeh, J., Horváth, I.S., 2020. Dry
623 Anaerobic Co-Digestion of Citrus Wastes with Keratin and Lignocellulosic
624 Wastes: Batch And Continuous Processes. *Waste and Biomass Valorization* 11,
625 423–434. <https://doi.org/10.1007/s12649-018-0447-y>

626 Peultier, P., 2016. Dispositif pour la méthanisation par voie sèche de matière
627 comprenant du fumier. EP 3 1117 39 A1.

628 Riggio, S., Hernández-Shek, M.A., Torrijos, M., Vives, G., Esposito, G., Van
629 Hullebusch, E.D., Steyer, J.P., Escudié, R., 2017a. Comparison of the mesophilic
630 and thermophilic anaerobic digestion of spent cow bedding in leach-bed reactors.
631 *Bioresour. Technol.* 234, 466–471. <https://doi.org/10.1016/j.biortech.2017.02.056>

632 Riggio, S., Torrijos, M., Debord, R., Esposito, G., van Hullebusch, E.D., Steyer, J.P.,
633 Escudié, R., 2017b. Mesophilic anaerobic digestion of several types of spent
634 livestock bedding in a batch leach-bed reactor: substrate characterization and
635 process performance. *Waste Manag.* 59, 129–139.

636 <https://doi.org/10.1016/j.wasman.2016.10.027>

637 Rocamora, I., Wagland, S.T., Villa, R., Simpson, E.W., Fernández, O., Bajón-
638 Fernández, Y., 2020. Dry anaerobic digestion of organic waste: A review of
639 operational parameters and their impact on process performance. *Bioresour.*
640 *Technol.* 299, 122681. <https://doi.org/10.1016/j.biortech.2019.122681>

641 Samaniuk, J.R., Wang, J., Root, T.W., Scott, C.T., Klingenberg, D.J., 2011. Rheology
642 of concentrated biomass. *Korea Aust. Rheol. J.* 23, 237–245.
643 <https://doi.org/10.1007/s13367-011-0029-z>

644 Schneider, N., Gerber, M., 2020. Rheological properties of digestate from agricultural
645 biogas plants: An overview of measurement techniques and influencing factors.
646 *Renew. Sustain. Energy Rev.* 121, 109709.
647 <https://doi.org/10.1016/j.rser.2020.109709>

648 van Soest, P.J., 1963. Use of Detergents in the Analysis of Fibrous Feeds. II. A Rapid
649 Method for the Determination of Fiber and Lignin. *J. Assoc. Off. Agric. Chem.* 46,
650 825–835.

651 Wu, B., 2014. CFD simulation of gas mixing in anaerobic digesters. *Comput. Electron.*
652 *Agric.* 109, 278–286. <https://doi.org/10.1016/j.compag.2014.10.007>

Figure captions

Fig. 1 Schematic diagram of developed pilot PFR for D-AD treatment

Fig. 2 (a) Experimental set-up, sampling campaign and physical and rheological analysis of raw SCM and digested samples **(b)** Visual aspect of samples taken from different PFR axial lengths

Fig 3. %TS, %VS, flash BMP and fiber content (hemicellulose, cellulose and lignin) evolution in sacrificed batch D-AD reactors **(a)** and in PFR **(b)** treating SCM

Fig 4. Evolution of yield stress in sacrificed batch D-AD reactors and in PFR

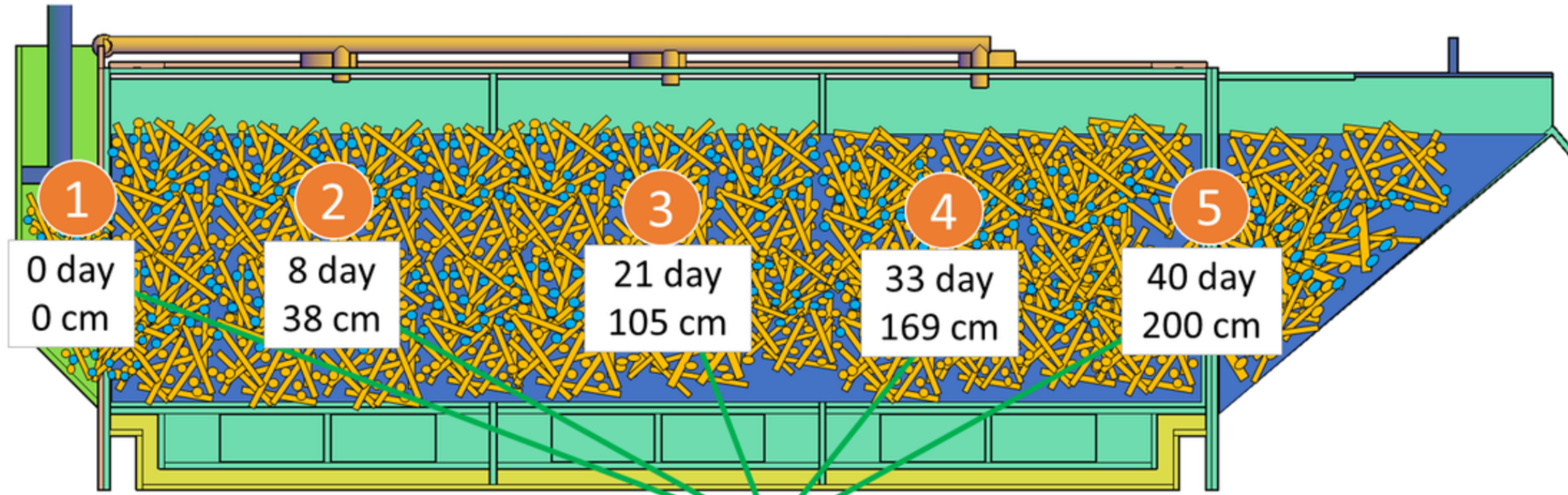
Fig 5. (a) Shear test at different normal efforts of the SCM **(b)** Constructed Morh-Coulomb failure diagram for SCM **(b)** cohesion evolution and **(c)** friction angle evolution during D-AD

Fig 6. (a) Specific biogas flow in PFR in Cycles 1 and 2 **(b)** Accumulated biogas and methane **(c)** Hypothetical biogas flow from each feed of SCM inside the continuous reactor with a residence time of 40 days and the resulted total flow

Table 1. Linear regression comparing the results of yield stress and the solid degradation in batch reactors

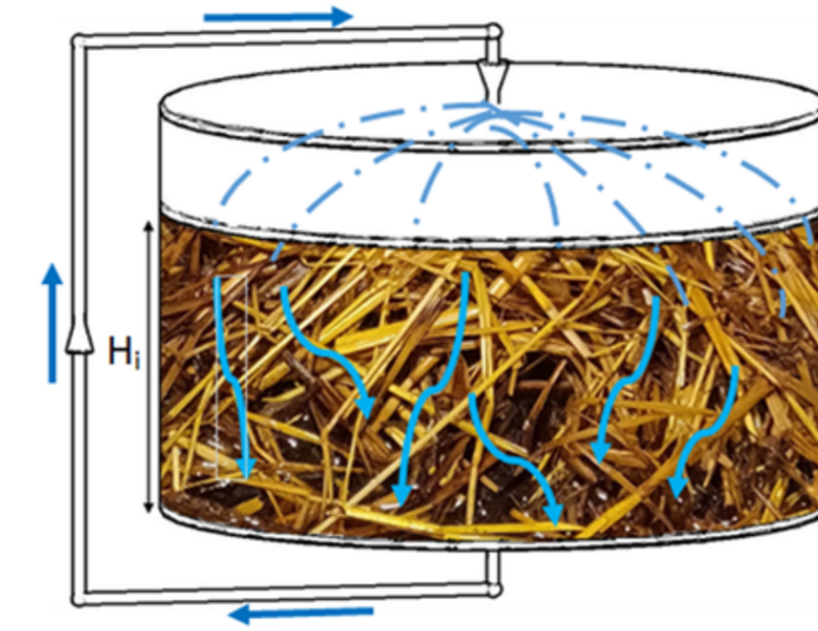
Table 2. Experimental results obtained with the shear-box

PLUG FLOW REACTOR 500 L 2 m of effective length



Samples from different points at the end of a solid retention time of 40 days

4 SACRIFICED LEACH BED REACTORS (60 L)

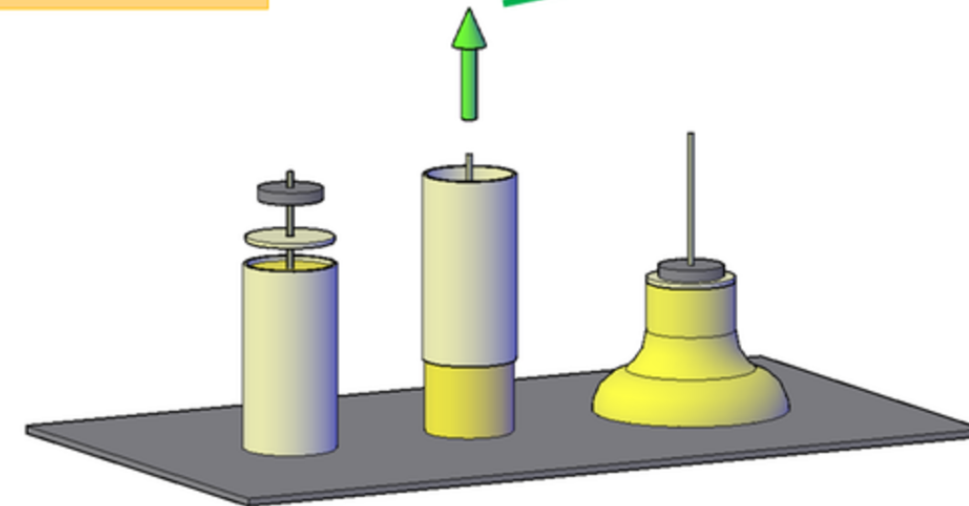


Samples from sacrificed reactors 0, 10, 21 and 31 days

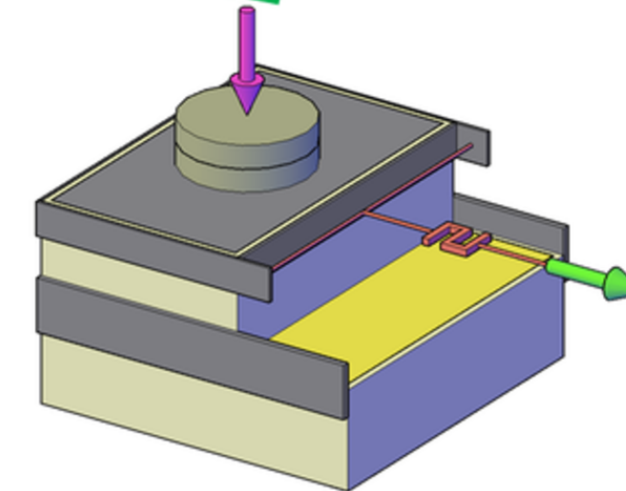
Physical and rheological characterization

%TS, %VS, Fiber content, Flash BMP[®]

Slump Test and Shear-box



Yield Stress



Cohesion and Friction Angle